

# Multifunctional supramolecular polymer networks as next-generation consolidants for archaeological wood conservation

Zarah Walsh<sup>a</sup>, Emma-Rose Janeček<sup>a</sup>, James T. Hodgkinson<sup>b,c</sup>, Julia Sedlmair<sup>d,e,f</sup>, Alexandros Koutsioubas<sup>g</sup>, David R. Spring<sup>b</sup>, Martin Welch<sup>c</sup>, Carol J. Hirschmugl<sup>f,h</sup>, Chris Toprakcioglu<sup>i</sup>, Jonathan R. Nitschke<sup>b</sup>, Mark Jones<sup>j</sup>, and Oren A. Scherman<sup>a,1</sup>

<sup>a</sup>Melville Laboratory for Polymer Synthesis, Department of Chemistry, University of Cambridge, Cambridge CB2 1EW, United Kingdom; <sup>b</sup>Department of Chemistry, University of Cambridge, Cambridge CB2 1EW, United Kingdom; <sup>c</sup>Department of Biochemistry, University of Cambridge, Cambridge CB2 1QW, United Kingdom; <sup>d</sup>US Forest Service, US Department of Agriculture, Forest Products Laboratory, Madison, WI 53276; <sup>e</sup>Department of Agriculture and Biological Engineering, Pennsylvania State University, University Park, PA 16802; <sup>f</sup>Synchrotron Radiation Center, Stoughton, WI 53589; <sup>g</sup>Forschungszentrum Jülich GmbH, Jülich Centre for Neutron Science at Heinz Maier-Leibnitz Zentrum, D-85747 Garching, Germany; <sup>h</sup>Department of Physics, University of Wisconsin–Milwaukee, Milwaukee, WI 53211; <sup>i</sup>Department of Physics, University of Patras, Patras 26500, Greece; and <sup>j</sup>The Mary Rose Trust, HM Naval Base, Portsmouth PO1 3LX, United Kingdom

Edited by Lee A. Newsom, Pennsylvania State University, University Park, PA, and accepted by the Editorial Board October 1, 2014 (received for review April 29, 2014)

**The preservation of our cultural heritage is of great importance to future generations. Despite this, significant problems have arisen with the conservation of waterlogged wooden artifacts. Three major issues facing conservators are structural instability on drying, biological degradation, and chemical degradation on account of Fe<sup>3+</sup>-catalyzed production of sulfuric and oxalic acid in the waterlogged timbers. Currently, no conservation treatment exists that effectively addresses all three issues simultaneously. A new conservation treatment is reported here based on a supramolecular polymer network constructed from natural polymers with dynamic cross-linking formed by a combination of both host-guest complexation and a strong siderophore pendant from a polymer backbone. Consequently, the proposed consolidant has the ability to chelate and trap iron while enhancing structural stability. The incorporation of antibacterial moieties through a dynamic covalent linkage into the network provides the material with improved biological resistance. Exploiting an environmentally compatible natural material with completely reversible chemistries is a safer, greener alternative to current strategies and may extend the lifetime of many culturally relevant waterlogged artifacts around the world.**

supramolecular polymer | conservation | waterlogged archaeological wood | Mary Rose

The 16th century *Mary Rose* was a marvel of her time, a world-class warship with state-of-the-art weaponry. She sank in battle in 1545 and lay submerged for more than 400 y until she was raised in 1982 (1, 2). Centuries underwater have caused many complications in her preservation, as the cellulosic components of the wood cells have been severely damaged from waterlogging and biological action by marine organisms (3, 4). The production of acid within the timbers (5, 6) from localized Fe<sup>3+</sup> deposits is a third contributor to the loss of cellulose, but has yet to be adequately addressed by conservation technologies (7, 8).

For the last 20 y, the ship's timbers have been sprayed continuously with increasing concentrations of aqueous poly(ethylene glycol) (PEG; maximum 50 vol.%) containing a broad spectrum biocide. This treatment aims to support the cell walls, preventing collapse, whereas the biocide hinders biological growth. Although PEG is easily applied, nontoxic, and inexpensive, a number of significant disadvantages exist for the conservation process. The need for lengthy treatment makes PEG application costly (9); additionally, PEG acts as a solid-state ion transporter (10), enabling the movement of acidic salts and iron through the timbers, creating more widespread chemical degradation issues. Finally, the action of bacteria, Fe<sup>3+</sup>, natural acids, temperature, and humidity on PEG can cause its degradation

to acidic byproducts over time (9). It is clear from the examination of PEG consolidants that another conservation strategy is necessary (11).

Recently, alternative consolidants have appeared in the literature with the focus moving toward oligoamides and natural polymers such as chitosan, guar, and 2-hydroxyethyl cellulose (11–14). These consolidants represent renewable and environmentally friendly alternatives to PEG with no acidic degradation products, enhanced timber compatibility, and a significantly reduced cost as they are often sourced as waste products from industrial processes. Despite such benefits, these materials alone do not offer a method of reducing or trapping Fe<sup>3+</sup>.

Through a straightforward chemical functionalization of chitosan and guar and addition of a macrocyclic host molecule, cucurbit[8]uril (CB[8]), a new supramolecular polymer network was developed for the conservation of waterlogged wooden artifacts that simultaneously addresses the three major issues facing conservators (Fig. 1). Chitosan was selected because of its

## Significance

**The preservation of cultural heritage is of widespread importance all over the world. Yet the lack of development in the field of conservation treatments means the fate of some of the most culturally important artifacts in the world remain in jeopardy. In the preservation of waterlogged wooden artifacts, conservators rely almost exclusively on poly(ethylene glycol) doped with a broad-spectrum biocide. The concept of a chemotactic consolidant, one that can adapt to the artifact it is treating, as described here has never before been described for an archaeological/conservation treatment. Additionally, the cross-links holding the consolidant together are entirely reversible, resulting in a material that is a greener, safer, and sustainable alternative to current conservation strategies.**

Author contributions: Z.W., J.R.N., M.J., and O.A.S. designed research; Z.W., E.-R.J., J.T.H., J.S., and A.K. performed research; Z.W., E.-R.J., J.T.H., and J.S. contributed new reagents/analytic tools; Z.W., J.T.H., J.S., A.K., D.R.S., M.W., C.J.H., and C.T. analyzed data; Z.W., E.-R.J., and O.A.S. wrote the paper; and D.R.S., M.W., C.J.H., C.T., M.J., and O.A.S. supervised research.

The authors declare no conflict of interest.

This article is a PNAS Direct Submission. L.A.N. is a guest editor invited by the Editorial Board.

See Commentary on page 17700.

<sup>1</sup>To whom correspondence should be addressed. Email: oas23@cam.ac.uk.

This article contains supporting information online at [www.pnas.org/lookup/suppl/doi:10.1073/pnas.1406037111/-DCSupplemental](http://www.pnas.org/lookup/suppl/doi:10.1073/pnas.1406037111/-DCSupplemental).



consolidants on the timbers (11, 25). Although none of the constituent materials of the polymer are themselves extraordinary or novel, the interaction of the various units and their assembly to form a multifunctional chemotactic consolidant material is completely innovative, to both this field and supramolecular chemistry in general, and results in a consolidant material that addresses the three most pressing issues facing conservators of waterlogged archaeological timbers.

## Results and Discussion

Confirmation of iron and sulfur deposits in the ship's hull (*Quercus rober*) was shown by scanning electron microscopy–energy-dispersive X-ray (SEM-EDX) (*SI Appendix, Figs. S3 and S4*). Formation of acid (oxalic, sulfuric, formic) can be attributed to both chemical and biological factors related to  $\text{Fe}^{3+}$  saturation (26). Chemical degradation relies on the catalytic activity of  $\text{Fe}^{3+}$ , present in high concentrations from corrosion of bolts used in the ship's construction 500 y ago. The  $\text{Fe}^{3+}$  is capable of mediating the conversion of elemental sulfur in the wood (mainly from anaerobically reduced seawater sulfates) to sulfuric acid (8). Naturally occurring oxalates in oak can be converted to oxalic acid through Fenton-type processes (6, 27). Biological degradation occurs through an anaerobic sulfur-reducing bacteria (genus *Desulfovibrio* and *Desulfomaculatum*) present in the timbers, which also generates sulfuric acid (26, 28). Both chemical and biological routes lead to damage of the cellulosic materials. Saturation of the timber with  $\text{Fe}^{3+}$  may be addressed by washing small artifacts with solutions of iron chelators (7); although promising in the laboratory, such techniques are impractical for artifacts the size of the *Mary Rose*. Unlike previous conservation treatments, the functional supramolecular polymer network presented here could trap  $\text{Fe}^{3+}$  preventing its catalytic activity.

Three four-component polymer systems were examined; in all cases, the first guest polymer was MV-BA guar, whereas the second guest polymer was either catechol (PolyCat), naphthol (PolyNap), or a 50:50 mixture of catechol and naphthol functionalized chitosan (PolyCatNap). The ability of PolyCat, PolyNap, and PolyCatNap to chelate and trap  $\text{Fe}^{3+}$  was first determined visually by addition of  $\text{Fe}_2(\text{SO}_4)_3$  ( $\text{Fe}^{3+}$ ) or  $\text{FeSO}_4$  ( $\text{Fe}^{2+}$ ) to each polymer solution (9 mM in water). On addition of  $\text{Fe}^{3+}$ , PolyCat and PolyCatNap changed from orange-brown to green-brown, whereas PolyNap became more intensely orange. The green hue indicated the formation of a catechol– $\text{Fe}^{3+}$  complex, whereas the intense orange color was likely due to an interaction between the free amines of the chitosan and  $\text{Fe}^{3+}$ . A similar orange color was observed in all samples on addition of  $\text{Fe}^{2+}$ , as amines preferentially bind to  $\text{Fe}^{2+}$ , whereas catechol has no interaction.

Introducing  $\text{Fe}^{3+}$  to the PolyCatNap sample yielded an additional structuring effect to the polymer network by providing more cross-links between the polymer chains through metal–ligand interactions. This enhanced cross-linking was illustrated by a simple inverted vial test (*SI Appendix, section S.7*) and confirmed by small angle X-ray scattering (SAXS; Fig. 2A). Such an effect was not observed in the PolyCat or PolyNap systems, as the formation of any metal–ligand interactions would in turn reduce the number of cross-links from the CB[8] ternary complexation in the PolyCat and cannot occur in PolyNap. Comparison of PolyCatNap by SAXS before and after addition of  $\text{Fe}^{3+}$  indicates that PolyCatNap behaves as a microparticulate gel with large particles solubilized in a polymer matrix (*SI Appendix, section S.6*) in the absence of  $\text{Fe}^{3+}$  (29–33). At pH 6.5, the gel particles are likely due to H-bonding between chitosan chains, which would not be expected of guar below pH 9, leaving guar as the solubilizing matrix. When  $\text{Fe}^{3+}$  was added, the particulate nature of PolyCatNap diminished and an enhanced polymer network formed.

Ordering was achieved by a combination of metal–ligand and ternary complex cross-links through the host–guest system.

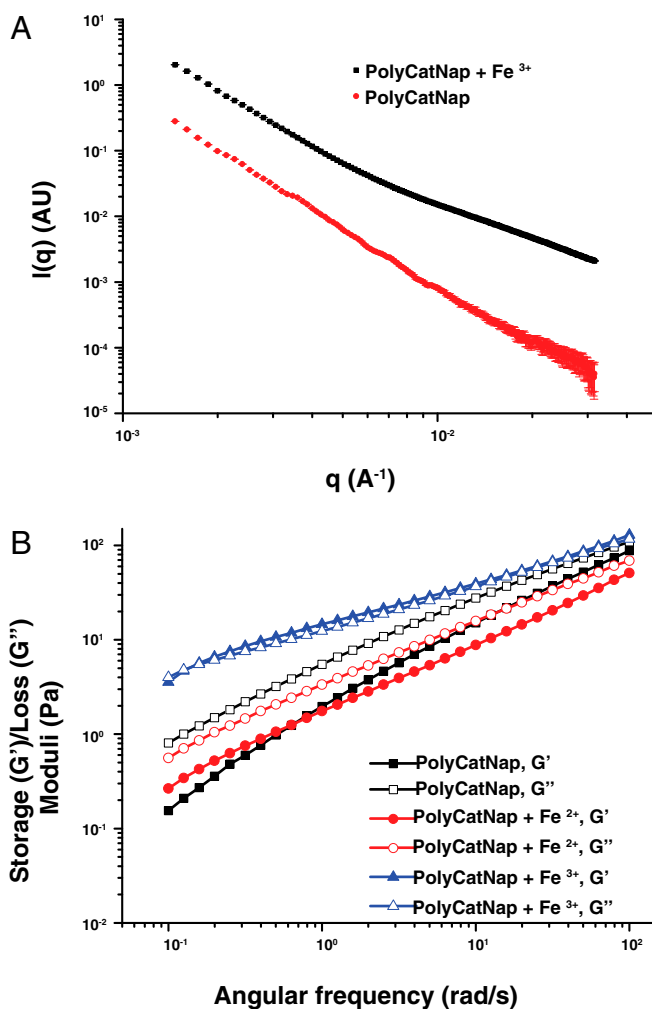


**Fig. 2.** Effect of iron on the polymer network. (A) SAXS data showing the change in the structure of the networks in the presence (black line) and absence (red line) of  $\text{Fe}^{3+}$ . (B) Angular frequency (rad/s) vs. storage ( $G'$ )/loss ( $G''$ ) moduli for PolyCatNap (black), PolyCatNap with  $\text{Fe}^{3+}$  (red), and PolyCatNap with  $\text{Fe}^{2+}$  (blue).

Visual inspection of the samples coupled with SAXS data confirmed that PolyCatNap readily and selectively binds  $\text{Fe}^{3+}$ , one of the three development criteria for a new consolidant.

Rheological studies were carried out on PolyCat, PolyNap, PolyCatNap, and their constituent materials. Data obtained were compared with the currently used consolidants PEG200 and PEG2000 (11). At standard concentrations, there was little difference in the viscosity of unfunctionalized guar, chitosan, and PEG solutions. The PolyCat, PolyNap, and PolyCatNap materials, however, have a significantly enhanced solution viscosity and shear strength. On addition of  $\text{Fe}^{3+}$ , PolyCatNap (Fig. 2B) and PolyCat (*SI Appendix, Fig. S8*) transition from gel-like materials to gels, with  $G' \geq G''$  over almost the entire shear range (three decades). This response is ideal as wood cells in the vicinity of  $\text{Fe}^{3+}$  deposits will likely be the most damaged on account of a high local acid concentration. In contrast, all three polymer networks displayed a decrease in viscosity on addition of  $\text{Fe}^{2+}$  (Fig. 2B). Such a chemotactic phenomenon is critical for the use of these materials as consolidants; when  $\text{Fe}^{3+}$  is absent, the material flows readily (through the timbers), and secondary cross-links form only when  $\text{Fe}^{3+}$  is encountered with concomitant in situ strengthening of the material.

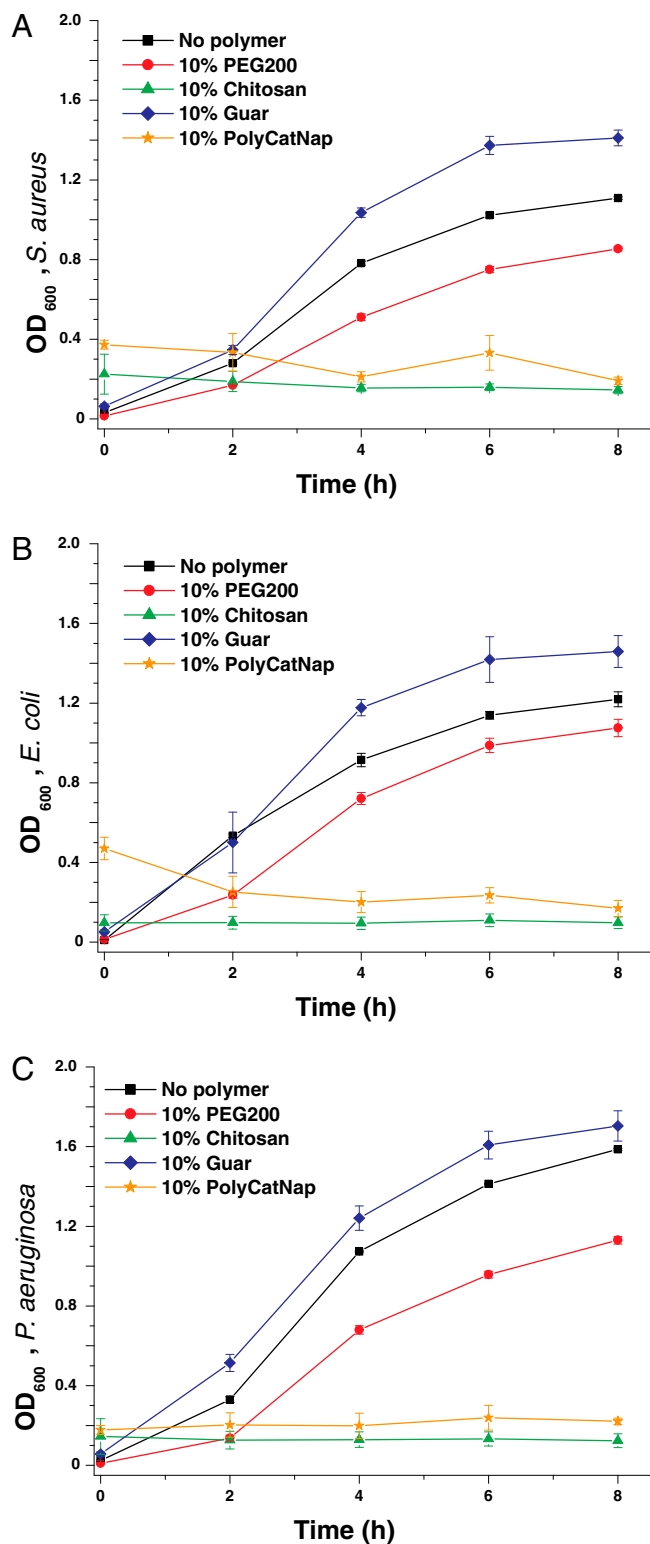


**Fig. 3.** Biological resistance of the polymer network. Activity of the negative control (black), PEG200 (red), chitosan (green), guar (blue), and PolyCatNap (orange), all at 10% (vol/vol), against bacterial growth, is shown in plots of time (h) vs. OD<sub>600nm</sub> for (A) *Staphylococcus aureus*, (B) *Escherichia coli*, and (C) *Pseudomonas aeruginosa*.

Rheology and SAXS indicated that the PolyCatNap system showed the best structural enhancement with iron chelation and was subjected to biological resistance tests. To determine the

effect of PolyCatNap on bacterial growth, three species were cultured in the presence of PolyCatNap and suitable controls in Mueller–Hinton broth [10% (vol/vol); Fig. 3]. The bacterial species tested were gram-negative *Pseudomonas aeruginosa* (34) and *Escherichia coli* and gram-positive *Staphylococcus aureus*, all detected in the timbers of the *Mary Rose*. Growth was monitored every 2 h according to a previously described method (35) (SI Appendix, section S.9).

Growth of all three species was inhibited in the presence of both PolyCatNap and chitosan over an 8-h period. Intriguingly, growth was enhanced by unfunctionalized guar relative to the negative control. It is noteworthy that, although PolyCatNap does contain guar, bacterial growth is still completely inhibited, likely due to the presence of the MV-BA moiety. Although growth was moderately reduced by PEG200 compared with the negative control, complete inhibition was only observed in the presence of chitosan, a known antibacterial agent (36), and PolyCatNap. The mode of action of PolyCatNap is unknown, yet it could potentially be exhibiting a dual antibacterial effect by (i) the strong chelation of iron, which is essential for bacterial metabolism and survival; and (ii) the presence of the antibacterial MV in the polymer backbone. Biological studies combined with rheological and SAXS data confirmed that PolyCatNap fulfills all three idealized criteria for a new consolidant material and has the potential to be a significant improvement on the state-of-the-art PEG treatments.

Understanding the long-term aging behavior of this new consolidant material is extremely important to its future use. Performing accelerated aging experiments is a convenient method of obtaining information on the degradation behavior of the material in a reduced amount of time (9). Because of the sensitivity of the CB[8] complex to temperatures in excess of 60 °C (reversibility of the handcuff effect at elevated temperatures), it was not possible to conduct a standard aging experiment with this material, such as described by Mortensen et al. (9). We have, however, recently studied the degradation behavior of unfunctionalized natural polymers and found no negative effects of the accelerated aging compared with PEG (11). To understand long-term behavior of these materials, particularly the effect of the natural degradation of the wood on the material, more than 10 pieces of previously untreated waterlogged oak from the *Mary Rose* in 1 × 1 × 0.25-cm dimensions were treated with the new conservation materials. These pieces will be observed regularly over the coming months and years for changes in the appearance of the timber to provide more information on the long-term behavior of these new consolidants.

Consolidant infiltration of timbers is also a long-term process, requiring months to years to extract meaningful results. Shorter-term experiments can, however, be useful to determine whether PolyCatNap might realistically replace PEG in the treatment of waterlogged archaeological timbers. Both high-resolution Fourier transform infrared (FT-IR) imaging and surface treatment experiments were carried out on sections of an oak (*Q. rober*) supporting beam and an oak chisel handle (raised with the *Mary Rose*), respectively.

Analysis with the Infrared Environmental Imaging (IRENI) beamline of 10- $\mu$ m-thick untreated and PolyCatNap-treated samples showed that similarities exist in the characteristic cellulose (1,347–1,400  $\text{cm}^{-1}$ ) and lignin (1,486–1,529  $\text{cm}^{-1}$ ) regions as expected; however, the samples exhibited distinctly different intensities in the N–H region (1,630–1,690  $\text{cm}^{-1}$ ) (37–40). As the chitosan polymers have a high N–H content, it is deduced that this increase in intensity signified the presence of chitosan polymers in the wood cells. Interestingly, hotspots appeared in the characteristic cellulose region in the PolyCatNap-treated sample, which are not present before treatment. These hotspots are likely due to the presence of the boronic ester (MV-BA) whose characteristic signals occur in the same region as cellulose. The

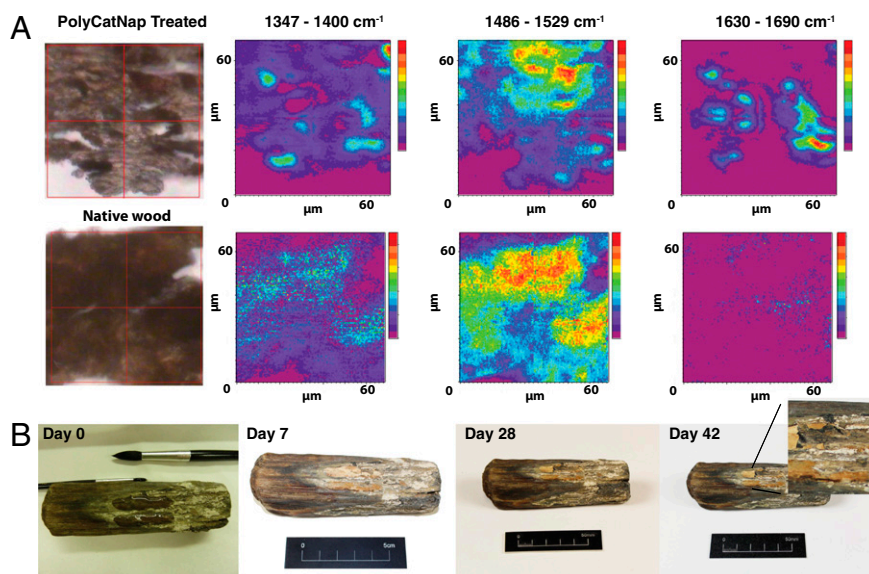


**Fig. 4.** Treatment of *Mary Rose* timbers. (A) Optical microscope (Left) and images of integration over specific spectral regions (Right) from high-resolution FT-IR imaging that shows the characteristic signals of cellulose (1,347–1,400  $\text{cm}^{-1}$ ) and lignin (1,486–1,529  $\text{cm}^{-1}$ ) in both treated and untreated wood and those of chitosan (1,630–1,690  $\text{cm}^{-1}$ ) in the PolyCatNap-treated sample, on a high-low absorbance scale where violet is low and red is high. (B) Photographic images of the treatment with PolyCatNap (1) and pure chitosan (2) of a chisel handle found on board the *Mary Rose* with significant surface iron deposits over a period of 6 wk, (Inset) with removal of the treatment to leave a cleaned artifact surface.

IR data confirmed that the PolyCatNap infiltrated the damaged timbers where it acted as a three-pronged consolidant, conferring structural stability and bacterial protection to the wood while acting as an  $\text{Fe}^{3+}$  scavenger. Additionally, analysis of the treated sample exhibited only a 30% shrinkage in the PolyCatNap-treated sample (*SI Appendix*, Fig. S9) compared with more than 50% without any treatment. Even after such a short treatment, noticeable improvements are observed in the artifact, which is a promising outcome of these preliminary tests.

Finally, the PolyCatNap system also showed great promise as a surface treatment on artifacts with significant surface iron deposits. Solutions of PolyCatNap and unfunctionalized chitosan [4% (wt/vol)] were applied to visible iron deposits on an oak chisel handle (Fig. 4B). Within 1 wk of drying, the PolyCatNap had incorporated a significant amount of the surface iron into the functional network and began delaminating from the artifact surface. In fact, it was possible to manually remove the surface salt layer through the self-assembled network material without damaging the artifact or leaving behind any visible residue; moreover, after 22 mo of visual observation, no surface salts have reappeared. Chitosan alone did not provide sufficient surface treatment confirming the need for the multicomponent PolyCatNap system.

## Conclusion

The combination of SAXS, IR imaging, rheology, and biological testing along with evaluation of surface treatment clearly shows the designed functional supramolecular polymer network can simultaneously address the three major issues facing conservators of waterlogged wooden artifacts. Although long-term studies to elucidate the diffusion of these materials in larger artifacts are necessary, the PolyCatNap system already represents a real and quantifiable advantage over current PEG treatments. With the relative ease of polymer functionalization, tailoring the dynamic network to address other issues in conservation science such as Fe/Cu inclusions in wood, leather, and bone and degradation of iron-gall inks in precious manuscripts is imminently possible. Additionally, with similar chemical functionalities, aqueous-based multifunctional orthogonal supramolecular

polymer systems such as PolyCatNap have the potential to expand beyond conservation into the treatment of metal-based blood disorders (hemochromatosis and thalassaemias). Thus, the system can be readily tuned and the true power of supramolecular self-assembly realized and appreciated by the general public.

## Materials and Methods

**Synthesis of 1-(4-Boronobenzyl)-1'-Methyl-[4,4'-Bipyridine]-1,1'-Diium.** 1-Methyl-4,4'-bipyridinium was first synthesized from 4,4'-bipyridine from a standard literature method. Following this, (4-(bromomethyl)phenyl)boronic acid (100 mg, 0.47 mmol) and 1-methyl-4,4'-bipyridinium (120 mg, 0.40 mmol) were dissolved in acetonitrile (4 mL), and the solution was heated to reflux overnight. The resulting red solid was isolated by filtration and recrystallized from ethanol, containing a few drops of water, to yield a red solid (132.2 mg, 0.28 mmol, 70%). Further details of all syntheses are given in the *SI Appendix*, *SI Materials and Methods*.

**Preparation of Biopolymers.** Guar (20 g) was stirred in water (2 L, 50 °C) overnight. The resulting suspension was centrifuged at  $1424 \times g$  for 2 min, and the supernatant was precipitated from ethanol, isolated by filtration, dried under vacuum, and ground to yield a white powder. For each functionalization experiment, chitosan was prepared fresh using the general procedure that 3 wt.% chitosan (~720 mg) was stirred in 1 vol.% acetic acid (~20 mL) at pH 6 until all of the chitosan was dissolved, and a viscous yellow liquid was obtained. This liquid was then added into the reaction vials to be functionalized with pendant guest molecules.

**Functionalization of Chitosan with PolyCat or PolyNap.** Either 3,4-dihydroxyphenylacetic acid (HPAA) or 2-naphthylacetic acid (NPAA) was stirred for 24 h with 1-ethyl-3-(3-dimethylaminopropyl)carbodiimide (EDC) in an equimolar ratio to aminate the carboxylic acid of the HPAA or NPAA. After 24 h, a 3 wt.% solution of chitosan in 1 vol.% acetic acid was added to the guest solution in a molar ratio of 0.2:1 (functional group:chitosan) and stirred for a further 72 h to attach the aminated guest molecule to the free amine on the chitosan backbone. After 72 h, the polymer was precipitated from solution using a 10 wt.% solution of NaOH, which was then filtered and washed with copious amounts of water (~3 L) to return the pH to neutral. The material was then collected and frozen in dry ice and then lyophilized for 72 h before use.

**Formation of the Gel-Like Consolidant Materials.** Gels were prepared by weighing 10 mg of guar, 1 mg of MV-BA, 30 mg of the HPAA-CS or NPAA-CS

(or a 1:1 mixture of the two polymers), and 4 mg of CB[8] into a clean vial and solvating in 4 mL of a 1 vol.% solution of acetic acid by stirring overnight on a magnetic stirring plate. Once prepared, the HPAA-containing gels appeared brown/orange in color, whereas the NPAA-containing gels were white, and combination gels were an opaque, beige color.

**Preparation of Samples for Analysis on the IR Beamline.** Samples were prepared by placing a 1 × 1 × 0.25-cm piece of supporting beam in the PolyCatNap solution for 1 wk, followed by storage in a sealed environment for 1 wk, and finally freeze-dried to remove water. Ten-micrometer slices of these samples were cut with a microtome and laid flat on standard glass microscope slides for analysis.

1. Bell LS, Thorp JAL, Elkerton A (2009) The sinking of the Mary Rose: A medieval mystery solved? *J Arch Sci* 36(1):166–173.
2. Millard AR, Schroeder H (2010) 'True British Sailors': A comment on the origin of the men of the Mary Rose. *J Arch Sci* 37(4):680–682.
3. Bjurhager I, et al. (2012) State of degradation in archeological oak from the 17th century Vasa ship: Substantial strength loss correlates with reduction in (holo)cellulose molecular weight. *Biomacromolecules* 13(8):2521–2527.
4. Bjordal CG, Nilsson T, Daniel G (1999) Microbial decay of waterlogged archaeological wood found in Sweden applicable to archaeology and conservation. *Int Biodeterior Biodegradation* 43(1-2):63–73.
5. Almkvist G, Persson I (2008) Degradation of polyethylene glycol and hemicellulose in the Vasa. *Holzforchung* 62(1):64–70.
6. Almkvist G, Persson I (2008) Fenton-induced degradation of polyethylene glycol and oak holocellulose. A model experiment in comparison to changes observed in conserved waterlogged wood. *Holzforchung* 62(6):704–708.
7. Fors Y, Sandström M (2006) Sulfur and iron in shipwrecks cause conservation concerns. *Chem Soc Rev* 35(5):399–415.
8. Sandström M, et al. (2002) Deterioration of the seventeenth-century warship Vasa by internal formation of sulphuric acid. *Nature* 415(6874):893–897.
9. Mortensen MN, Egsgaard H, Hvilsted S, Shashoua Y, Glastrup J (2007) Characterisation of the polyethylene glycol impregnation of the swedish warship Vasa and one of the Danish Skuldev Viking ships. *J Arch Sci* 34(8):1211–1218.
10. Gray FM (1997) *Polymer Electrolytes, RSC Materials Monographs* (Royal Society of Chemistry, Cambridge, UK).
11. Walsh Z, Janeček E-R, Jones M, Scherman OA (2014) Natural polymers as alternative consolidants for the preservation of waterlogged archaeological wood. *Stud Conservat*. 10.1179/2047058414Y.0000000149.
12. Cipriani G, Salvini A, Baglioni P, Bucciarelli E (2010) Cellulose as a renewable resource for the synthesis of wood consolidants. *J Appl Polym Sci* 118(5):2939–2950.
13. Cipriani G, Salvini A, Fioravanti M, diGiulio G, Malavolti M (2013) Synthesis of hydroxylated oligoamides for their use in wood conservation. *J Appl Polym Sci* 127(1):420–431.
14. Christensen M, Kutzke H, Hansen FK (2012) New materials used for the consolidation of archaeological wood – past attempts, present struggles, and future requirements. *J Cult Herit* 13(3):5183–5190.
15. Chenite A, Buschmann M, Wang D, Chaput C, Kandani N (2001) Rheological characterisation of thermogelling chitosan/glycerol-phosphate solutions. *Carbohydr Polym* 46(1):39–47.
16. Lehn J-M (2002) Toward self-organization and complex matter. *Science* 295(5564):2400–2403.
17. de Greef TFA, Meijer EW (2008) Materials science: Supramolecular polymers. *Nature* 453(7192):171–173.
18. Zhang J, et al. (2012) One-step fabrication of supramolecular microcapsules from microfluidic droplets. *Science* 335(6069):690–694.
19. Service RF (2005) How far can we push chemical self-assembly? *Science* 309(5731):95.
20. del Barrio J, et al. (2013) Photocontrol over cucurbit[8]uril complexes: Stoichiometry and supramolecular polymers. *J Am Chem Soc* 135(32):11760–11763.
21. Kim HJ, et al. (2001) Selective inclusion of a hetero-guest pair in a molecular host: Formation of stable charge-transfer complexes in cucurbit[8]uril. *Angew Chem Int Ed Engl* 40(8):1526–1529.
22. Appel EA, et al. (2010) Supramolecular cross-linked networks via host-guest complexation with cucurbit[8]uril. *J Am Chem Soc* 132(40):14251–14260.
23. Rauwald U, Biedermann F, Deroo S, Robinson CV, Scherman OA (2010) Correlating solution binding and ESI-MS stabilities by incorporating solvation effects in a confined cucurbit[8]uril system. *J Phys Chem B* 114(26):8606–8615.
24. Rauwald U, Scherman OA (2008) Supramolecular block copolymers with cucurbit[8]uril in water. *Angew Chem Int Ed Engl* 47(21):3950–3953.
25. Bardet M, Gerbaud G, Tran QK, Hediger S (2007) Study of interaction between polyethylene glycol and archaeological wood components by C-13 high-resolution solid-state CP-MAS NMR. *J Arch Sci* 34(10):1670–1676.
26. May E, Jones M (2008) *Molecular Bacterial Diversity in the Timbers of the Tudor Warship the Mary Rose. Heritage Microbiology and Science: Microbes, Monuments and Maritime Materials* (Royal Society of Chemistry, Cambridge, UK), pp 204–218.
27. Almkvist G, Persson I (2008) Analysis of acids and degradation products related to iron and sulfur in the Swedish warship Vasa. *Holzforchung* 62(6):694–703.
28. Berko A, et al. (2009) XAS studies of the effectiveness of iron chelating treatments of Mary Rose timbers. *J Phys Conf Ser* 190:012147.
29. Horkay F, Hecht A-M, Mallam S, Geissler E, Rennie AR (1991) Macroscopic and microscopic thermodynamic observations in swollen poly(vinyl acetate) networks. *Macromolecules* 24(10):2896–2902.
30. Pezron I, Djabourov M, Leblond J (1991) Conformation of gelatin chains in aqueous solutions: 1. A light and small-angle neutron scattering study. *Polymer* 32(17):3201–3210.
31. Debye P, Bueche A (1949) Scattering by an inhomogeneous solid. *J Appl Phys* 20:518–525.
32. Koberstein JT, Picot C, Benoit H (1985) Light and neutron scattering studies of excess low-angle scattering in moderately concentrated polystyrene solutions. *Polymer* 26(5):673–681.
33. Mallam S, Horkay F, Hecht A-M, Geissler E (1989) Scattering and swelling properties of inhomogeneous polyacrylamide gels. *Macromolecules* 22(8):3356–3361.
34. Sun H-Y, Fujitani S, Quintiliani R, Yu VL (2011) Pneumonia due to *Pseudomonas aeruginosa*: Part II: Antimicrobial resistance, pharmacodynamic concepts, and antibiotic therapy. *Chest* 139(5):1172–1185.
35. Tokura S, Ueno K, Miyazaki S, Nishi N (1997) Molecular weight dependent antimicrobial activity by chitosan. *Macromol Symp* 120(1):1–9.
36. Raafat D, von Barga K, Haas A, Sahl H-G (2008) Insights into the mode of action of chitosan as an antibacterial compound. *Appl Environ Microbiol* 74(12):3764–3773.
37. Nasse MJ, et al. (2011) High-resolution Fourier-transform infrared chemical imaging with multiple synchrotron beams. *Nat Methods* 8(5):413–416.
38. Nasse MJ, et al. (2011) Multi-beam synchrotron infrared chemical imaging with high spatial resolution: Beam line realization and first reports on image restoration. *Nucl Instrum Methods Phys Res A* 649(1):172–176.
39. Hirschmugl CJ, Gough KM (2012) Fourier transform infrared spectrochemical imaging: Review of design and applications with a focal plane array and multiple beam synchrotron radiation source. *Appl Spectrosc* 66(5):475–491.
40. Kastyak-Ibrahim MZ, et al. (2012) Biochemical label-free tissue imaging with sub-cellular-resolution synchrotron FTIR with focal plane array detector. *Neuroimage* 60(1):376–383.